Quaternary International 602 (2021) 66–81

Contents lists available at ScienceDirect

Quaternary International

journal homepage: www.elsevier.com/locate/quaint

Using a multi-proxy approach to locate the elusive Phoenician/Persian anchorage of Tel Akko (Israel)

Matthieu Giaime [a,b,c,*], Harry M. Jol [d], Yossi Salmon [b,c], Gloria I. López [b,c], Amani abu Hamid [b,c,e], Logan Bergevin [d], Paul Bauman [f], Alastair McClymont [f], Ethan Sailer-Haugland [d], Michal Artzy [b,c]

[a] Institut de Ciència I Tecnologia Ambientals (ICTA-UAB), Universitat Autònoma de Barcelona, 08193 Cerdanyola Del Vallès, Barcelona, Spain
[b] Hatter Laboratory, Leon Recanati Institute for Maritime Studies, University of Haifa, Abba Khoushy Ave 199, Haifa, 3498838, Israel
[c] Department of Maritime Civilizations, The Leon. H. Charney School of Marine Sciences, University of Haifa, Abba Khoushy Ave 199, Haifa, 3498838, Israel
[d] Department of Geography & Anthropology, University of Wisconsin-Eau Claire, 105 Garfield Avenue, Eau Claire, WI, 54701, USA
[e] Israel Antiquities Authority, Rockefeller Archeological Museum, P.O.B 586, Jerusalem, 9100402, Israel
[f] BGC Engineering INC. Suite 500 - 1000 Centre St. NE, Calgary, AB, T2E 7W6, Canada

ARTICLE INFO

Keywords:
Anchorages/harbors
Geoarchaeology
Geomorphology
Ostracods
Sedimentology
Electrical resistivity tomography (ERT)
Ground penetrating radar (GPR)

ABSTRACT

Previous geoarchaeological research on the Akko coastal plain have contributed to the understanding of the ancient coastal interface and added evidence as to the location/shift of the ancient anchorages dating from the Middle Bronze Age (beginning of the 2nd Millennium BC) to the Early Hellenistic period (mid of the 2nd century BC) of the ancient site of Tel Akko. The present research provides new insights into the environmental changes and likely anchorage sites along the western edge of Tel Akko in the 1st Millennium BC (Iron Age II and III, periods associated with the Phoenician mariners and Persian army incursion). Our approach for locating the anchorage is based on a detailed investigation of subsurface sediments combining sedimentological and faunal analysis and radiocarbon dating of cores as well as identification of ceramic sherds found in the cores, and ground penetrating radar (GPR) and electrical resistivity tomography (ERT) surveys. Paleoenvironmental changes are compared and contrasted with the results of the archaeological investigations on the tell and in its vicinity. Our new data demonstrates that the Phoenician/Persian maritime interface of Tel Akko was mainly oriented toward the southwestern area of the tell where a natural anchorage was likely to have been located. At that time, the water depth in this area was ca. 2m, allowing for the anchorage of seagoing vessels. Increasing sediment deposition lead to the deterioration of direct, and eventual loss of access, to the sea. These conditions initiated the abandonment of the tell in the Early Hellenistic period as well as the westward shift to habitation on the peninsula, now the 'Old city of Akko', the Crusaders' Saint Jean d'Acre.

1. Introduction

The layout of ancient coastal cities is dictated by the shoreline position as well as any neighbouring river. In dynamic geomorphic settings, palaeoenvironmental reconstruction of ancient coastal settlements are particularly challenging unless a multi-disciplinary approach is taken. The natural anchorages or artificial harbours – lifelines of ancient coastal sites – may evolve or be relocated over time. This depends on the change in orientation of the coastline due to sea-level changes, sedimentary inputs, coastal erosion and associated hazards (Giaime et al., 2019). In the 3rd and 2nd Millennia BC, the eastern Mediterranean populations favoured natural coastal features as anchorage areas whereas artificial harbour basins and related port facilities started to be developed mainly during the Iron Age (Marriner et al., 2014, 2017). Along the coast of the southern Levant, the lack of bays on the coast, encouraged the utilizations of river-mouths for maritime activities during the Bronze Age (Raban, 1985, Fig. 1A). River-mouths have generally been used as safe havens for relatively short time periods. Over the long term they were vulnerable to a multitude of natural hazards, which include infilling by both fluvial and

* Corresponding author. Institut de Ciència I Tecnologia Ambientals (ICTA-UAB), Universitat Autònoma de Barcelona, 08193 Cerdanyola Del Vallès, Barcelona, Spain.
E-mail address: matthieu.giaime@gmail.com (M. Giaime).

https://doi.org/10.1016/j.quaint.2021.06.008
Received 31 August 2020; Received in revised form 31 May 2021; Accepted 6 June 2021
Available online 23 June 2021
1040-6182/© 2021 The Authors. Published by Elsevier Ltd. This is an open access article under the CC BY license (http://creativecommons.org/licenses/by/4.0/).

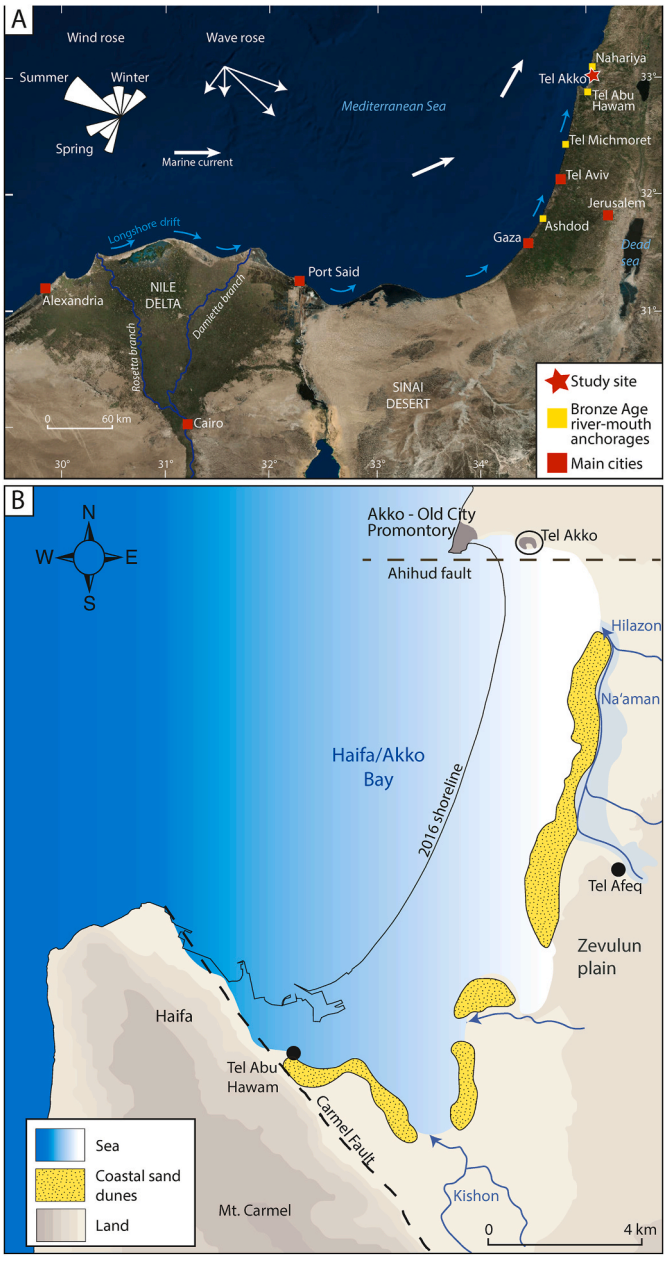


Fig. 1. A) General location of Haifa Bay in the southern Levant (after Inman, 2003; image ©CNES).
Dominant wind and wave patterns at Alexandria are shown in the rose diagrams (Stanley and Bernhardt, 2010). B) Geomorphological reconstruction of Haifa Bay 4000 years BP (after Elyashiv et al., 2016).

marine sediments due to sea level stabilisation (Giaime et al., 2019).

The UNESCO World Heritage site of Akko/Acre is one of the oldest continuously inhabited sites along the Levantine coast although its habitation pattern has evolved through time (general chronology given in Table 1). The main change occurred at the beginning of the Hellenistic period when the tell was deserted in favour of the Akko promontory where the city is presently situated (Artzy, 2015, Fig. 2).

The first archaeological remains at Tel Akko are dated to the beginning of the Early Bronze Age, ca. 5000 years ago. The first phase of urbanisation took place on the tell at the beginning of the Middle Bronze. An impressive rampart reaching a height of 22 m and a width of 60 m dated to the Middle Bronze IIa period was erected on the northern side of the tell. The highest part of it was located in Area AB, where a large MBII building was constructed (Dothan, 1976; Raban, 1983, 1991; Beeri, 2008, Fig. 3). The development of this urban centre deeply transformed the pre-existing forest ecosystems toward an urban environment with a vegetation biome dominated by cultivated species and urban weeds (Kaniewski et al., 2013). Written sources, including letters from the rulers of Akko, found mainly in Egypt, identifies the city as an important harbour town serving the Egyptian authorities in the mid-second Millennium BC (Artzy, 2012), although excavations have only located the latest part of the Late Bronze (late second Millennium BC) until now.

Table 1
Main historical periods of Tel Akko from the Bronze Age to the Hellenistic period.

Period	Years BC
Early Bronze	3500–2200
Middle Bronze	2200–1550
Late Bronze	1550–1200
Iron Age I	1200–1000
Iron Age II (Phoenician)	1000–586
Iron Age III (Persian)	586–332
Hellenistic	332–37

The second period of economic growth at Tel Akko is centred on the second part of the Iron Age including the Persian Period at which time, signs of iron works were noted. The habitation pattern and the population density increased after ca. 700-600 years BC (Artzy and Be'eri, 2010). The importance of Tel Akko in the trading network of the Levantine coast during the Iron Age is attested by the presence of Phoenicians, Persians and Greeks merchants (Gambash, 2014). It wasn't until the Hellenistic period (3rd and early 2nd century BC) that the centre of the town moved to the promontory, where the 'Old City of Akko/Acre is located (Artzy, 2015, Fig. 2).

By using a multidisciplinary geo-environmental approach, we aim to present the geomorphological setting of the western area of Tel Akko in the Iron Age where a marine environment has been evidenced in our previous research (Morhange et al., 2016; Giaime et al., 2018). We seek to determine the possibilities of an anchorage and associated environmental limitations for that area. The reconstruction of environmental changes affecting the western area of Tel Akko is fundamental for the understanding of the development of the tell as well as the evolution of the habitation patterns during the Phoenician/Persian period.

2. In search of Tel Akko's Phoenician/Persian anchorage: (geo) archaeological context

The coastal site of Tel Akko was founded on the northern limit of the Haifa/Akko Bay atop a naturally-occurring sand and *kurkar* feature. At Tel Akko, the *kurkar*, a local eolianite, is part of the Kurdane formation (Kafri and Ecker, 1964) which is pre-Pleistocene of age (Sivan et al., 1999). The site is located in a dynamic geomorphological environment at the end of the Nile's littoral cell and in the proximity of the Na'aman River (Belos) and its mouth (Morhange et al., 2016; Giaime et al., 2018, Fig. 1B). Haifa/Akko bay was formed by the subsidence of a geological graben delimited by two normal faults (Fig. 1B). It has undergone significant landscape changes during the Holocene (Zviely et al., 2006; Elyashiv et al., 2016, Fig. 1B). Following postglacial sea-level rise and subsequent flooding of the graben, the shoreline transgressed several kilometres to the east, reaching its maximum landward position ca. 4000 years ago (Zviely et al., 2006). During the past 4000 years, the coastline rapidly prograded to the west. The main driver of this progradation was the deposition of 700 million m^3 of Nile-derived quartz-rich sands transported northerly by longshore currents (Zviely et al., 2007) while fluvial sediment inputs from the local rivers appears as a secondary factor with exceptions for the northern and southern extremities of the bay where the two main coastal streams flow into the sea (Vachtman et al., 2013; Zviely et al., 2006).

An artificial 'Phoenician-style' harbour was identified following

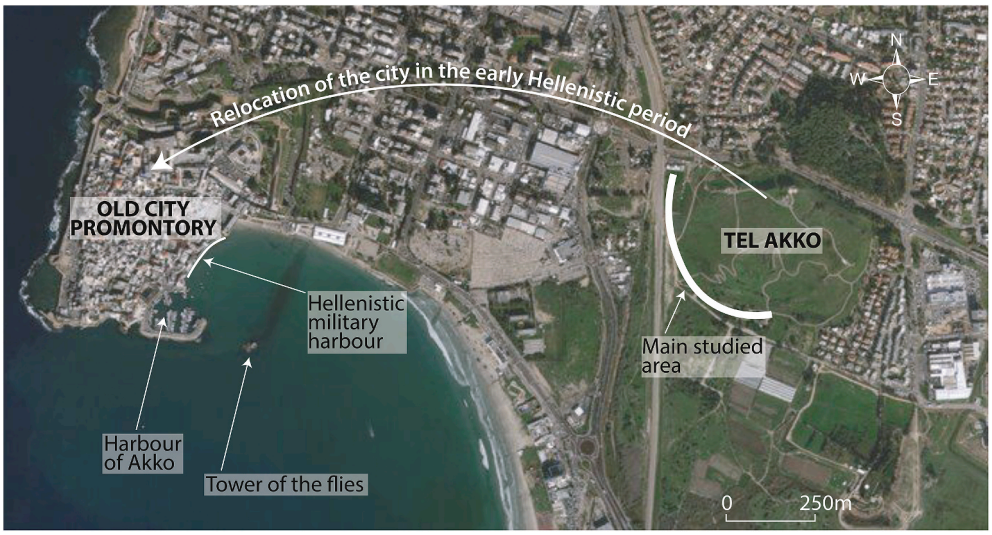


Fig. 2. Location of the main archaeological areas and main habitation centres cited in the text. Background image © Zoom Earth, Microsoft.

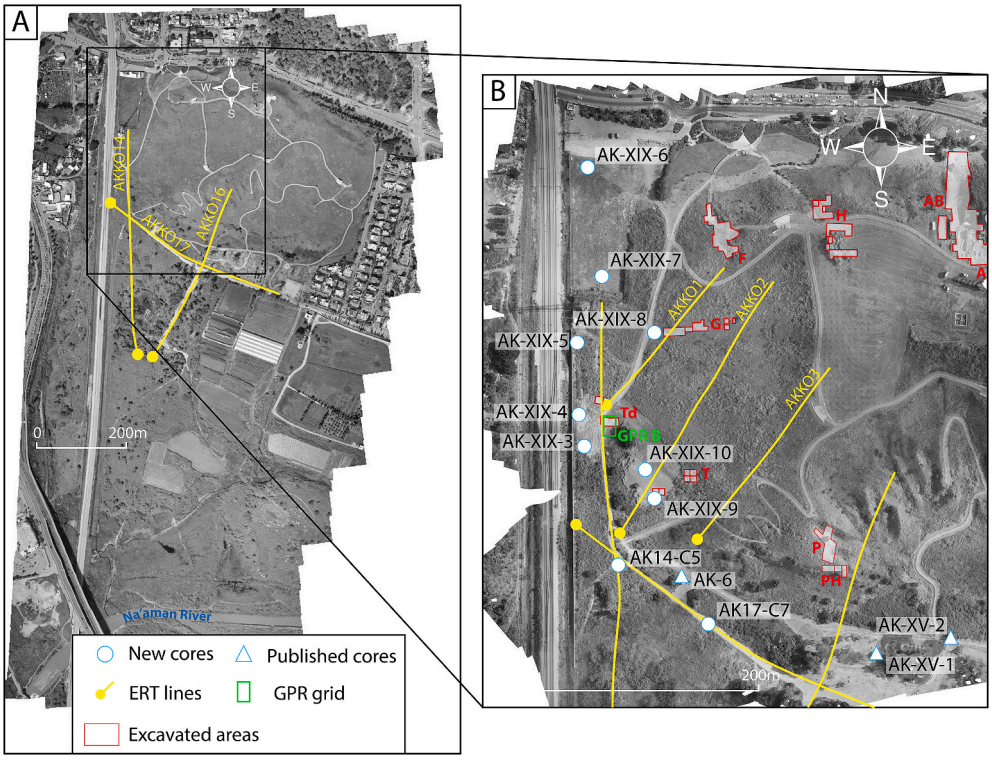


Fig. 3. A) Location map of ERT lines collected on Tel Akko southern plain (background image taken by drone © P. Bauman, 2018). B) Location map of the sedimentary cores, GPR grids (to add), ERT profiles and excavated areas at Tel Akko. Start of the ERT line (0m) is shown by the yellow dot (background image taken by drone © J. Quatermaine, 2019). (For interpretation of the references to colour in this figure legend, the reader is referred to the Web version of this article.)

submarine archaeological prospections around the 'Tower of flies' which is still a landmark feature in the Bay (Linder and Raban, 1965; Raban and Stieglitz, 1993, Fig. 2). It has been dated to the 6th century BC, the time of the of the Persian king, *Cambysis' incursion* during his conquest of Egypt. However, more recent studies have qualified this dating. Artzy (2012) proposes that 'Phoenician-type' harbours continued to be constructed in the south-eastern Mediterranean well after the Phoenician Period. One example is the harbour at Amathus, Cyprus (Empereur and Verlinder, 1987; Empereur, 1995; Empereur et al., 2018) which, despite depicting some Hellenic elements, was still constructed mainly in the Phoenician style around 300 BC. In addition, a re-study of the ceramics from Raban's excavations, have not shown any pre-Hellenistic ceramic evidence. In addition, archaeological excavations in the Akko promontory where the 'Old City' is located have not shed light on pre-Hellenistic occupation. Moreover, dredging of Akko's fishermen's harbour has not provided evidence for the presence of pre-Hellenistic material in the harbour basin (Galili et al., 2010; Galili and Rosen, 2017). Gambash (2014) states that during the mid 6th century BC of the Persian period, Akko did not serve as a logistical centre and regular *point d'appui* for Persian armies and fleets. It was only in the late 5th and 4th centuries BC that the Persian gathered their army of mercenaries at Tel Akko under Artaxerses II and III (Gambash, 2014;

Diodorus Siculus XV.41).

On Tel Akko, archaeological finds support the fact that the tell was the main centre of the area during the Persian period. On the summit of the tell (Area A, Fig. 3), a Phoenician *ostracon* (a potsherd used as a writing surface), the longest ever found in Phoenicia, was unearthed (Dothan, 1985a). More Phoenician *ostraca*, not yet published, were found in Area G, on the western side of the tell (Fig. 3), where a massive building was noted as well (Artzy and Quatermaine, 2014). The latest coins found in Area G are dated to the first half of the second century BC (Artzy, 2012). Rich remains from the Late Persian Period (late 5th-4th century BC) as well as numerous imports from the Aegean world were found during excavations (Artzy and Be'eri, 2010; Dothan, 1976, 1985b), especially in Area F in the north-western side of the tell (Raban, 1993, Fig. 3). Area T, also on the western side of the tell, was studied during a salvage excavation in 2010 directed by Abu Hamid of the Israel Antiquities Authority (IAA). Results showed the presence of a small industrial area dated to the 4th century BC, where Late Persian to Early Hellenistic ceramics were found (Artzy, 2012, Fig. 3), as well as a gravelly-sand facies bearing shells and ceramics interpreted as a high-energy coastline (Artzy, 2012). Pit surveys carried out, as part of the 'Total Archaeology' Project, directed by Killebrew and Artzy since 2010, accentuate the extent of 5th-4th century BC finds including an unusual large numbers of sherds, especially of Maritime Transport Containers, both local and imported.

Based on the above evidence, Tel Akko was a major commercial hub of the Mediterranean trade network in the Persian period, so it is hard to assume that its harbour was situated in the bay, 1.5 km from the main habitation and storage area.

3. Material and methods

Over the past ten years, geoarchaeological studies have shed light on the importance of fluvio-coastal changes and possible location of Tel Akko's anchorage(s) as early as the Middle Bronze Age (Morhange et al., 2016; Giaime et al., 2018; Artzy et al., 2021). The focus of this paper lays on the geomorphological evolution and the possibilities of anchorage on the western edge of the tell (Figs. 2 and 3). We carried out a detailed sub-surface multi-disciplinary investigation. Ground penetrating radar (GPR) and electrical resistivity tomography (ERT) surveys combined with sedimentological and faunal analysis of sedimentary cores. Cores were radiocarbon dated and ceramic sherds found in the cores were analysed to provide high-precision relative chronology. Sediment cores, GPR grids and ERT lines have been geographically located with a Differential Global Positioning System (DGPS) and altitude benchmarked relative to present mean sea level (msl) with a Total Station.

3.1. Electrical resistivity tomography (ERT)

The ERT profiles were collected in two phases: ERT profiles Akko-1, Akko-2, and Akko-3 were acquired in July 2011, and ERT profiles Akko-14, Akko-16, and Akko-17 were acquired in February 2018. The ERT profiles collected in 2011 were designed to investigate targets on the flanks of Tel Akko to depths of up to 20 m below ground surface (mbgs), and were acquired using an ABEM SAS 3000 resistivity system, a minimum electrode spacing of 1.5 m, and with standard Wenner array acquisition sequences. The 2018 profiles were designed to investigate deeper geological layers surrounding Tel Akko and were acquired with a multichannel ABEM Terrameter LS unit, a minimum electrode spacing of 5.0 m, and expanded gradient array acquisition sequences. Positions and topographic profiles for each ERT line were surveyed using handheld Trimble Geo XH GPS units, with a nominal accuracy in vertical and horizontal directions of less than 1 m.

For the 2011 and 2018 ERT surveys, resistivity data were collected through a linear array of electrodes coupled to a direct current (DC) resistivity transmitter and receiver, and an electronic switching box. The spacing between electrodes largely controls the horizontal and vertical resolution of the data (smaller spacing results in higher horizontal and vertical resolution). Similarly, the length of the array controls the depth of investigation (longer arrays yield greater investigation depths). Data collection was carried out in a sequential and automated fashion that takes advantage of all possible combinations of current injection and potential measurement electrodes. The data are downloaded to a computer for processing and analysis. The data were then inverted using a two-dimensional (2-D) finite difference or finite element inversion routine using the RES2DINV software. To enhance layer boundaries at shallow depths, the 2011 ERT profiles were inverted using a robust (L1-norm) constraint on the model. Conversely, due to lower resistivity contrasts between subsurface layers surrounding Tel Akko, a smooth model (L2-norm) constraint was used for the 2018 ERT profiles. The model output from each ERT line is a 2-D cross-section plotting resistivity (in ohm-m), versus depth. All ERT sections are presented as colour grids with warm colours (reds and pinks) indicating relatively high resistivities and cool colours (light and dark blues) showing regions of low resistivities.

3.2. Ground penetrating radar (GPR)

GPR can be used to investigate and identify human-made and/or geomorphic features based on the sediments' dielectric permittivity and electrical conductivity (Conyers and Goodman, 1997). GPR is a non-invasive near-surface geophysical surveying technique that uses electromagnetic waves to image the subsurface (Jol and Bristow, 2003).

A GPR survey was collected using a Sensors & Software pulseEKKO 1000 GPR system with an antennae frequency of 225 MHz (0.1 m step size and 0.5 m antenna separation). The grid dimensions were 24 m × 10.75 m (individual lines are 0.25 m apart). Site determination was based on archaeological excavations (Td) on the tell.

After grid collection occurred, GPR lines were imported into GFP_Edit 4 (GPR Files and Parameters) and an axis-based grid was created. The created GFP file is then exported to a Sensors and Software GPR processing application - EKKO_Project 5. GPR profiles were processed in a software extension called SliceView (gain adjusted between 7 and 8). Conductive sediments affected the average velocity for the grid and was calculated to be between 0.07 and 0.08 m/ns based on hyperbolic measurements.

3.3. Collection and analysis of the cores

Ten sediment cores were collected in plastic liners using a hydraulic percussion driller (Geoprobe DT22). Prior to split-opening and logging the sediment cores, every core section was initially run through a Multi-Sensor Core Logger (MSCL) (PetroLab facility, University of Haifa). Magnetic susceptibility (MS) measurements were key in deciphering between "natural" sedimentation (i.e., weak or negative MS values produced by diamagnetic properties of well sorted quartz sand layers; Thompson and Oldfield, 1986) and more anthropogenic-like signatures (characterised by fluctuating MS values mainly due to the presence of ceramics or changes in sediment texture). Core sub-samples from every stratigraphic unit were taken for micropaleontological and sedimentological analyses. General sediment texture, i.e., gravel (>2 mm), sand (63 μm–2 mm) and silty-clay fractions (<63 μm), was determined by wet-sieving. Ostracods were picked from the sand fraction >125 μm and identified using atlases and specific literature (Athersuch et al., 1989; Lachenal, 1989; Frenzel and Boomer, 2005; Avnaim-Katav et al., 2016). Molluscs were identified only from the gravel fraction (D'Angelo and Garguillo, 1978; Avnaim-Katav et al., 2016).

3.4. Chronology

Four samples (grape seeds and charcoals; Table 2) were radiocarbon dated by Accelerator Mass Spectrometry (AMS) at the Radiochronology Laboratory of the *Centre d'études nordiques* (University of Laval, Canada)

Table 2
AMS-14C data expressed in calibrated years BP and BC at the 95% confidence level (2σ). using Calib 8.2 (Stuiver and Reimer, 1993; Stuiver et al., 2020) and the IntCal20 curve (Reimer et al., 2020). amsl: above mean sea level.

Sample	Lab number	Material	Depth (cm below surface)	Elevation (cm amsl)	Age 14C	2 sigma cal. BP min; max	2 sigma cal. BC/AD min; max	Historical Period
AK-XIX-3578	ULA-8700	Charcoal	578	45 amsl	2800 ± 20	2850; 2960	1010; 900 BC	Early Iron Age
AK-XIX-4565	ULA-8695	Charcoal	565	106 amsl	2455 ± 15	2370; 2700	750; 420 BC	Late IA - Persian
AK-XIX-5678	ULA-8698	Charcoal	678	141 amsl	2455 ± 20	2370; 2700	750; 420 BC	Late IA - Persian
AK-XIX-5710	ULA-8697	Seed (grape)	710	106 amsl	2485 ± 20	2470; 2720	770; 520 BC	Late IA - Persian

and the Keck Carbon Cycle AMS Facility (University of California–Irvine, USA). Identification of several ceramic fragments recovered from the cores provides a high-precision relative chronology for specific stratigraphic units (Table 3).

4. Results

4.1. ERT measurements

ERT lines Akko-1, Akko-2 and Akko-3 were surveyed on the western slope of the tell (Figs. 3 and 4). They demonstrate the presence of a

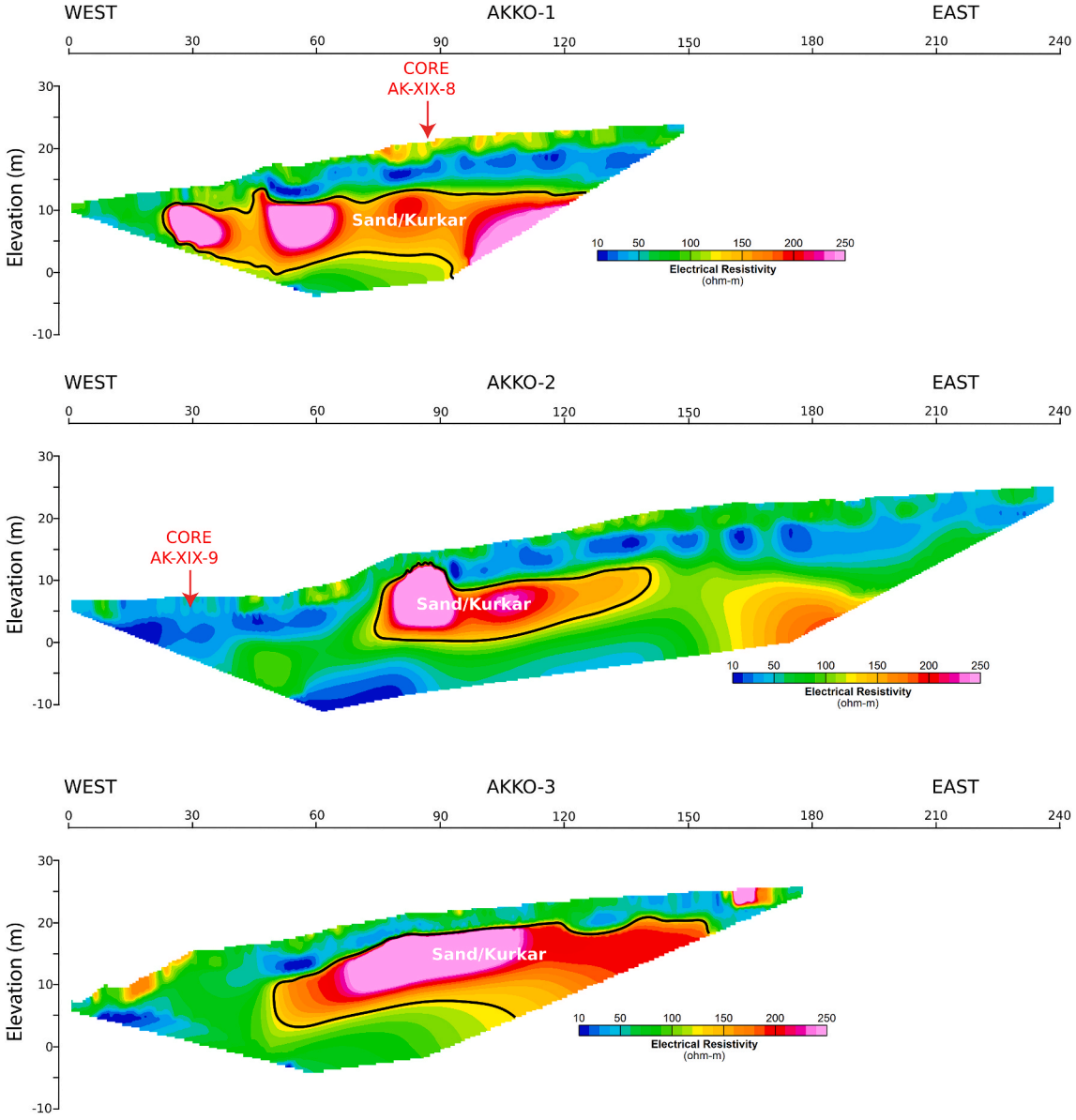


Fig. 4. ERT lines Akko-1, Akko-2 and Akko-3. The profiles were collected on the western edge of Tel Akko (see Fig. 3). Horizontal scale is 9.42 pixels per unit spacing. Vertical exaggeration = 1.23. High resistivity features attest of the presence of sands/kurkar sandstone.

relatively low to moderate resistive material (blue to green colours in the image) in the first 4–6 m below surface and interpreted as fine-grained sediments such as an anthropogenic/agricultural soil. Highly resistive features (>200 Ω-m; red to pink colours), interpreted as a *kurkar* outcrop or sandy unit (both exhibit the same high resistivity values in the ERT profiles) are shown deeper in the subsurface.

Three 450-500 m-long ERT lines were surveyed in order to map the subsurface sedimentary sequence of the coastal plain. Lines Akko-14 and Akko-16 have a mostly north/south orientation, whereas Akko-17 trends approximately west/east (Figs. 3 and 5). Most of the sections are dominated by a low resistivity (blue colour) material interpreted as fine-grained (fine sands and silty-clays) over-saturated sediments. Discrete, moderately resistive features are present at 10–20m depth. Only the northern part of ERT lines Akko-14 and Akko-16 shows high resistive material (pink colour) interpreted to be dry soil and colluvium from the tell, overlying *kurkar* sandstone (Fig. 5) although it is challenging to differentiate the nature of the subsurface sediments in this area as *kurkar*, dry sands and colluvium will exhibit the same high resistivity values (see Fig. 6).

4.2. GPR

Ground penetrating radar data was collected on the western portion of the tell (near Td excavation) where a coastal environment was

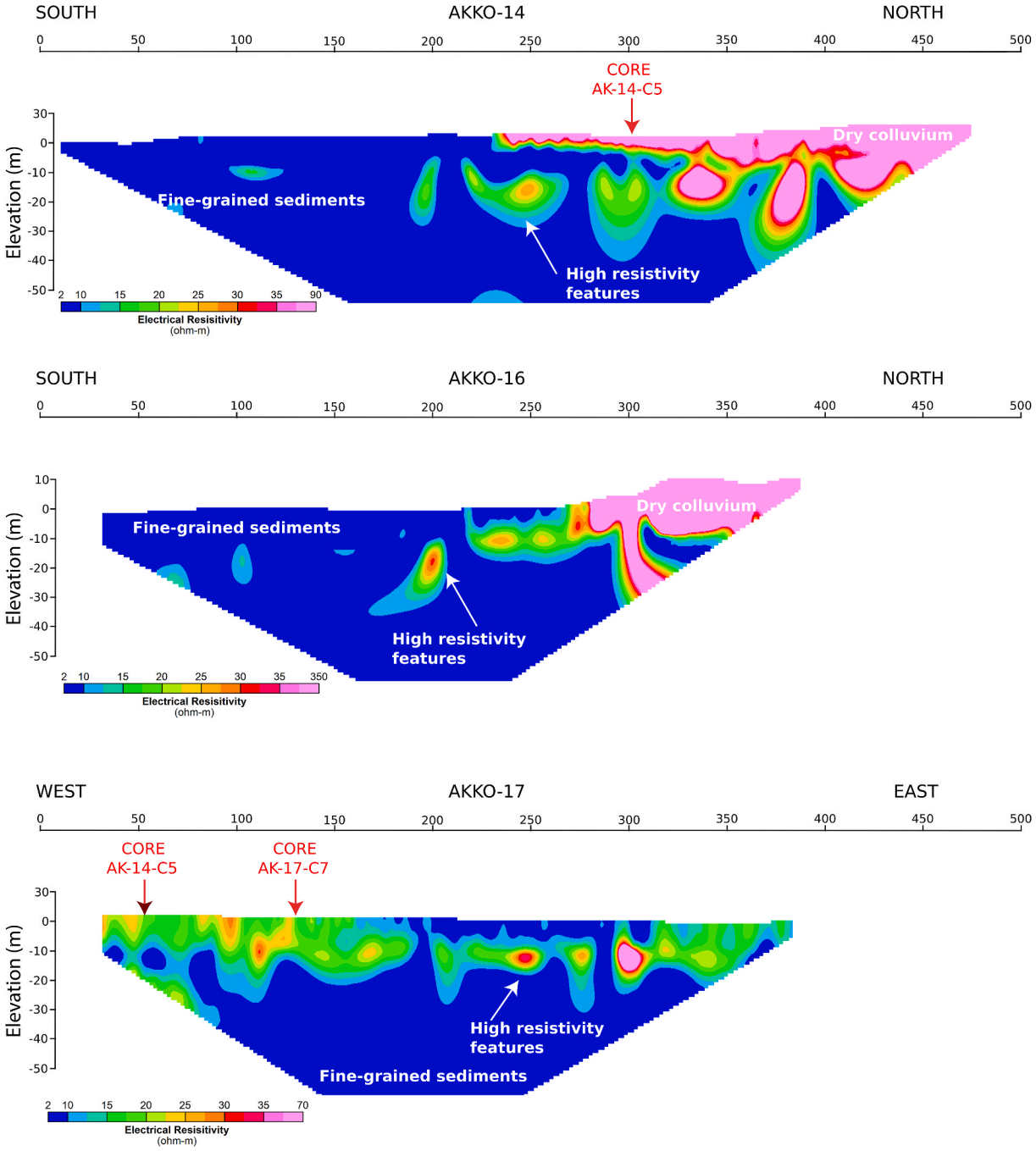


Fig. 5. ERT lines Akko-14, Akko-16 and Akko-17 collected on the Tel Akko coastal plain (see Fig. 3). Most of the sections are dominated by low resistivity (blue) material which are interpreted as fine over saturated sediments (silty-clay and fine sands). (For interpretation of the references to colour in this figure legend, the reader is referred to the Web version of this article.)

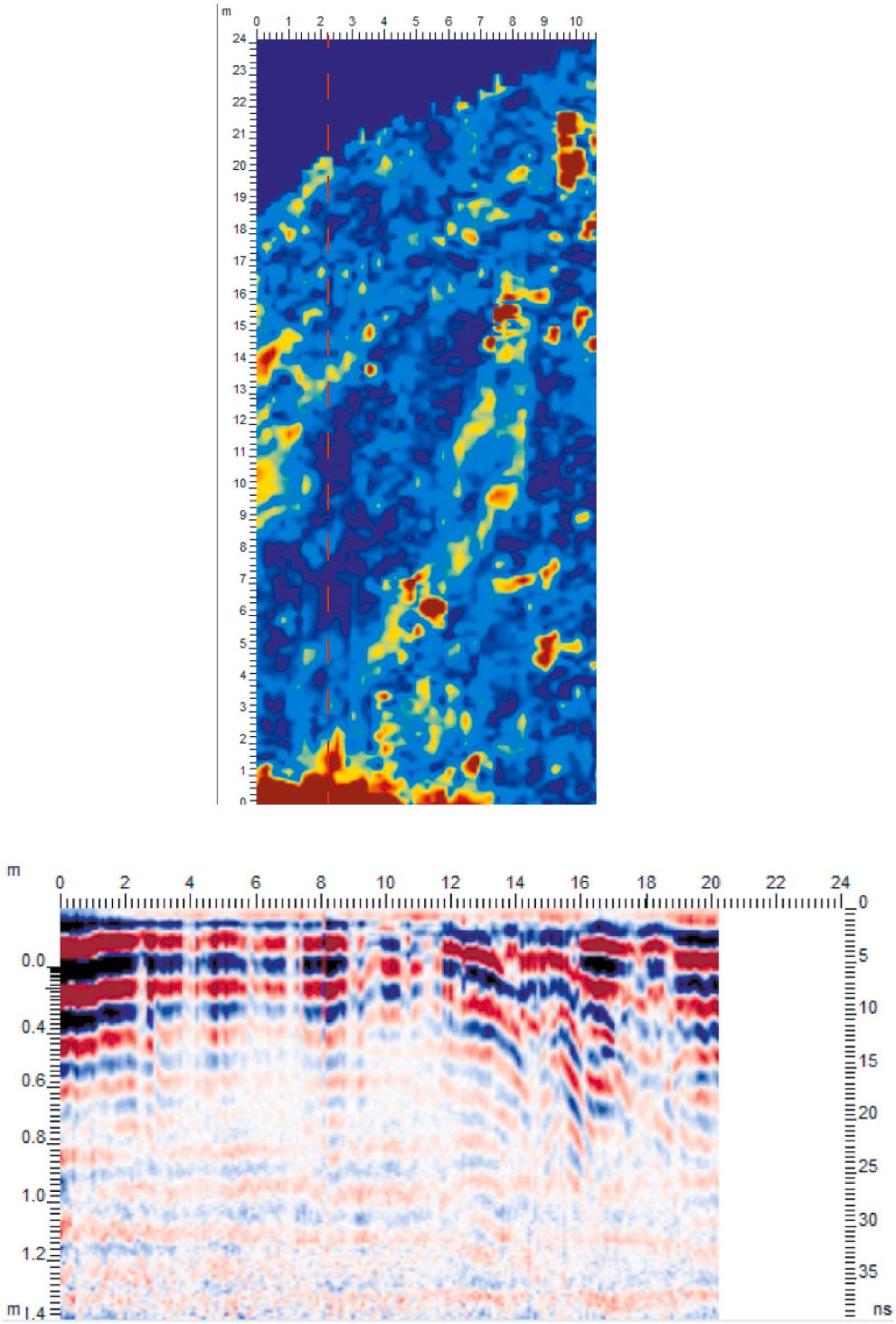


Fig. 6. Ground penetrating radar data was collected on the western portion of the tell (near Td excavation). The upper plan view image is a depth slice from 0.44 m to 0.55 m depth. A curvilinear feature is highlighted in this depth horizon. The lower image is Line 9 of the data collected. From 0 m to 12 m, multiple subhorizontal to horizontal continuous reflections become dipping reflections at 12 m–20 m.
The reflection pattens from the GPR data collected are interpreted as an aggradational and progradational geomorphic environment such as a coastline.

interpreted based on archaeological finds. The upper planview image is a depth slice from between 0.44 m and 0.55 m depth. A curvilinear feature is highlighted in this depth horizon. The lower image is individual Line 9 of the grid data. From 0 m to 12 m, multiple subhorizontal to horizontal continuous reflections become dipping reflections from 12 m to 20 m. The reflection pattens discovered within the GPR data collected are interpreted as an aggradational and progradational geomorphic environment such as a coastline.

4.3. Core analyses

Stratigraphic units were described for each of the 10 cores analysed for this study according to sedimentary texture and colour, MS properties and eventually faunal content. The environment identified for each stratigraphic unit is interpreted according to the Mediterranean benthic classification system (Pérès and Picard, 1964; Pérès, 1982; Figs.1 Supplementary Material) Analysis of the ceramic sherds found in the cores confirms the robustness of the radiocarbon chronology measurements, however, radiocarbon dating of one piece of charcoal shows a slight discrepancy that could be attributed to the old wood effect or the

reworking of older material (Sample ULA-8700; Table 2).

4.3.1. Core AK-XIX-8

Core AK-XIX-8 was drilled on the western slope of the tell, at an elevation of 14.30 m above mean sea level (amsl) and 90 m from the start of the ERT line Akko-1 (Figs. 3, 4 and 7). This site was selected to test the nature of the high resistivity features identified in the ERT profiles at >5m depth (Fig. 4). Two stratigraphic units are present in core AK-XIX-8.

Unit A (10–6 m depth), is composed of fine sands containing cm-scale *kurkar* aggregates. MS values are close to zero and constant, characteristic of well sorted fine aeolian quartz-rich sands, as confirmed by observation under the stereomicroscope.

Unit B (6–0 m depth) is dominated by brown silty-clay sediments with a subsidiary fraction of fine sands and some *kurkar* aggregates which is characteristic of an anthropogenic/agricultural soil. MS measurements show highly variable values due to the presence of small sherds and variable sediment texture.

4.3.2. Cores AK-XIX-6 and AK-XIX-7

AK-XIX-6, drilled at an elevation of 6.80 m amsl and AK-XIX-7 (7.33 m amsl) are the northernmost cores of this study (Figs. 3 and 8). The core was divided into three stratigraphic units.

Unit A, correspond to the substrate, located 860–750 cm below surface (180–70 cm below mean sea level; bmsl) in AK-XIX-6 and 750–620 cm below surface (17 cm bmsl–113 cm amsl) in AK-XIX-7. It is composed of fine to medium ochre-coloured quartz-rich sands containing cm-scale *kurkar* aggregates. This unit is characterised by negative magnetic susceptibility values (-10.10^-5 to -2.10^-5 SI for AK-XIX-6 and <-17.10^-5 SI for AK-XIX-7).

Unit B, is composed of clean yellow sands between 750 and 300 cm below surface in AK-XIX-6 (70 cm bmsl–380 cm amsl) and between 600 and 405 cm below surface in AK-XIX-7 (113–328 amsl). MS values are close to zero in AK-XIX-6 and slightly higher and less constant in AK-XIX-7 due to the presence of sherds. In AK-XIX-7, the top of unit B is dated from the Persian period and the sherds present sharp edges sign of an absence of wave action abrasion. Unit B is interpreted as a supralittoral

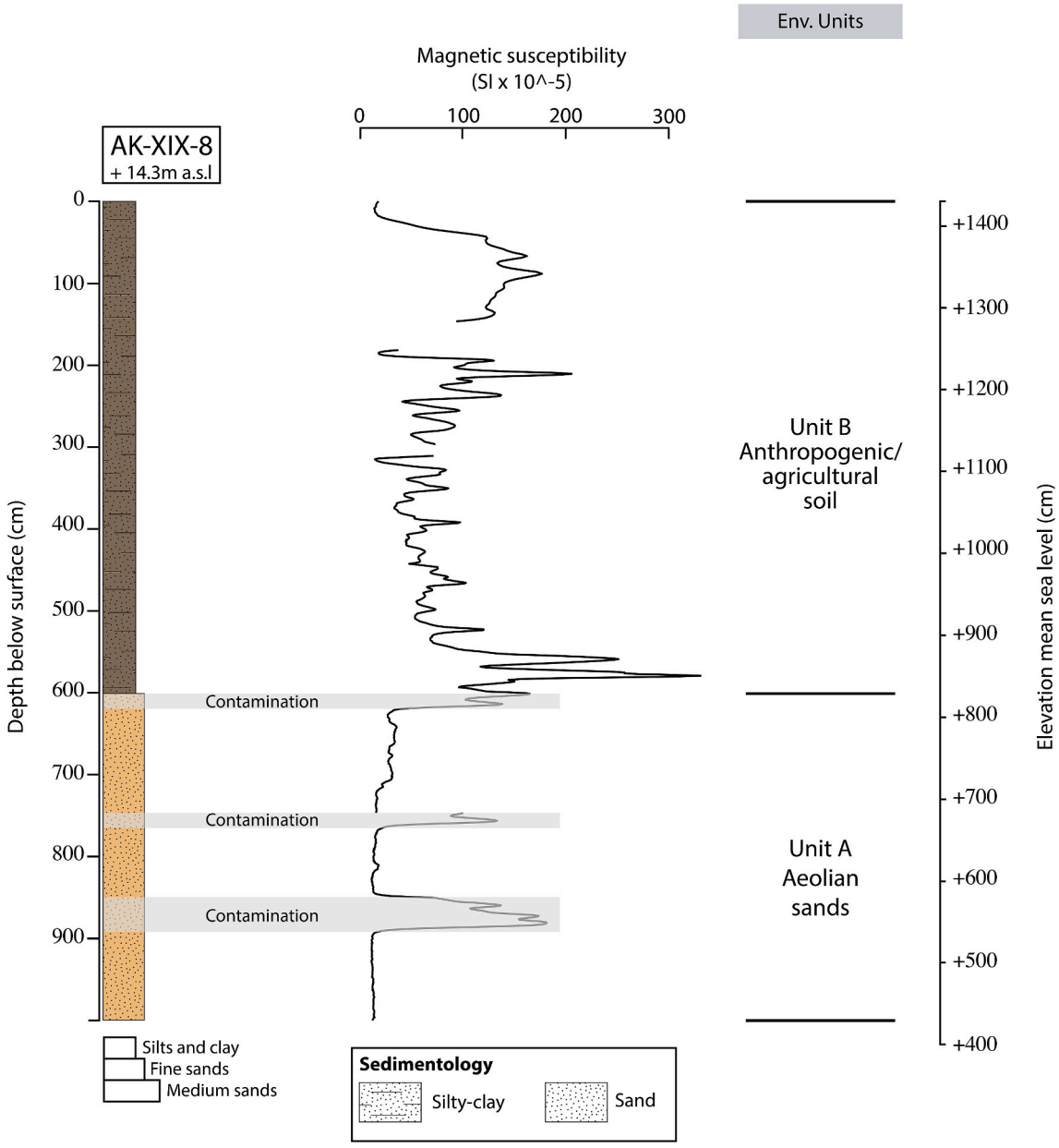


Fig. 7. Core AK-XIX-8. This sediment core shows the presence of two distinct stratigraphic units. See Fig. 3 for location of the core.

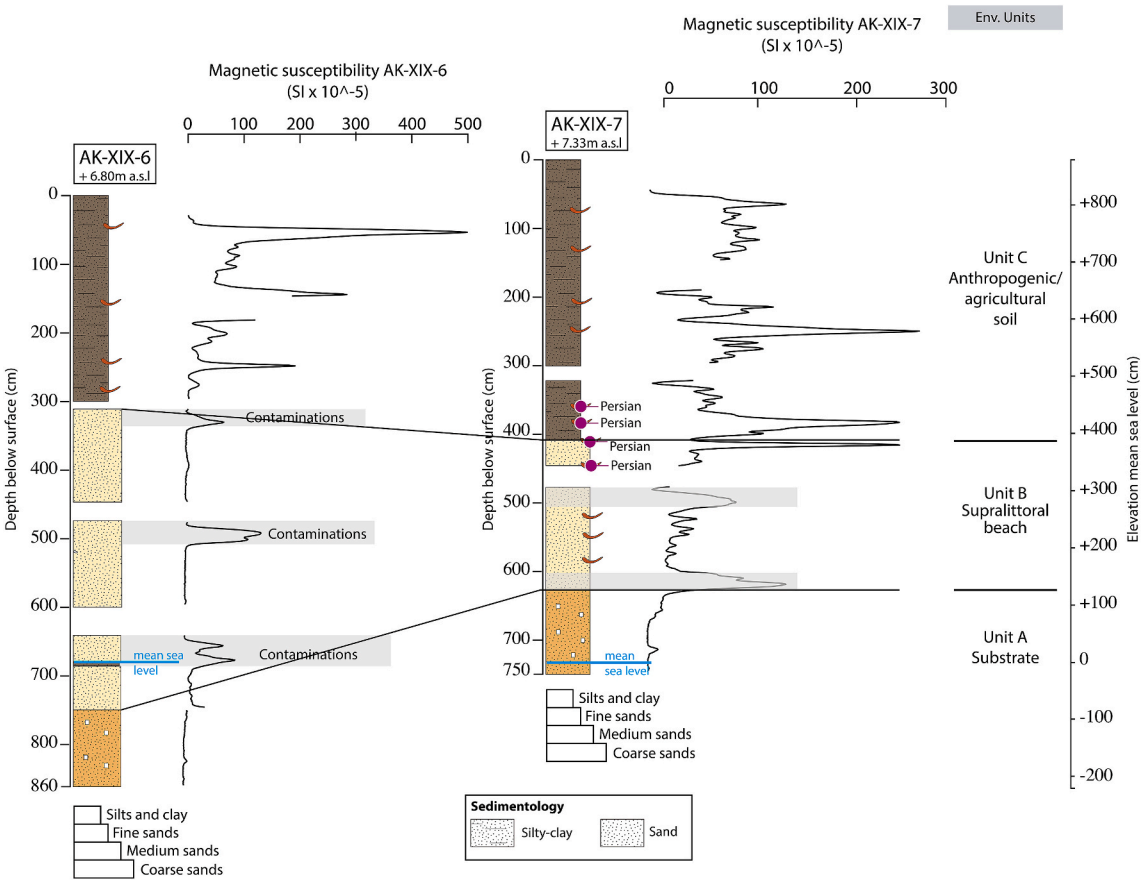


Fig. 8. Cores AK-XIX-6 and AK-XIX-7. The sediment cores show the presence of an supralittoral environment followed by the development of an agricultural soil. See Fig. 3 for location of the cores.

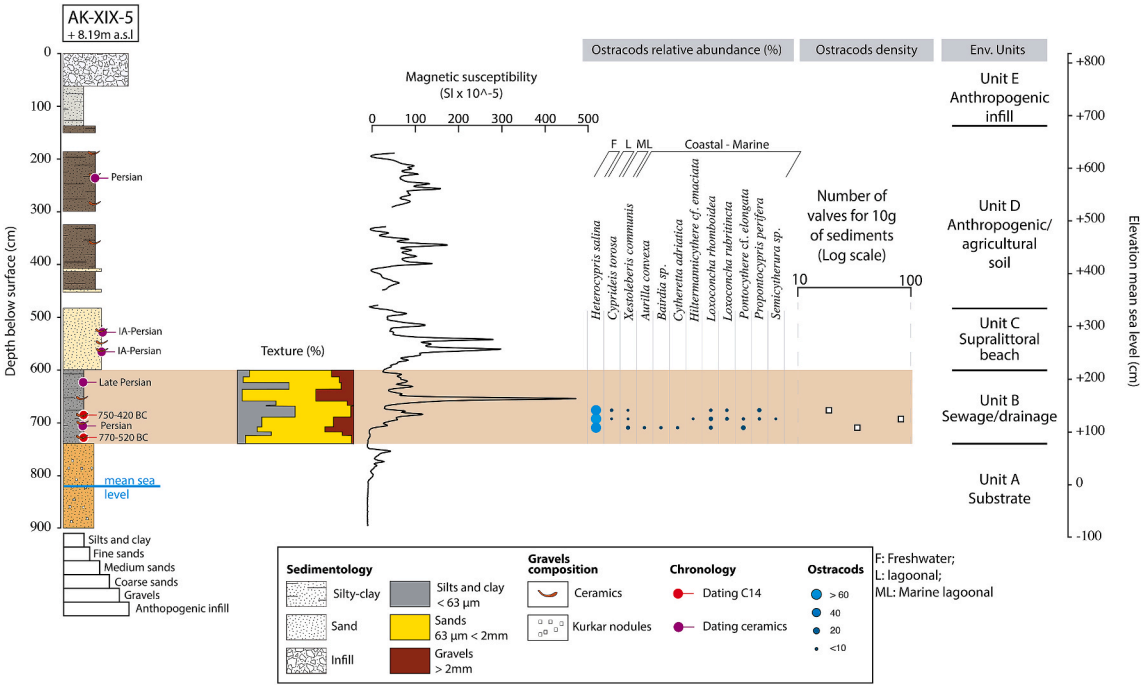


Fig. 9. Sedimentary texture, magnetic susceptibility and analysis of ostracods in core AK-XIX-5. Three different environmental units were identified. The unit highlighted in light brown show the sewage/drainage identified in this core. Fauna is dominated by the ostracod specie *Heterocypris salina*. See Fig. 3 for location of the core. (For interpretation of the references to colour in this figure legend, the reader is referred to the Web version of this article.)

environment.

Unit C, correspond to the uppermost unit of both cores. It is dominated by brown silty-clay sediments with a subsidiary fraction of fine sands and some *kurkar* aggregates. MS values range from 0.10^-5 to 500.10^-5 SI due to lithological and textural heterogeneity and the presence of small sherds. It is interpreted as an anthropogenic/agricultural soil.

4.3.3. Core AK-XIX-5

Core AK-XIX-5 was drilled at an elevation of 8.19 m amsl (Figs. 3 and 9). It can be divided into five different stratigraphic units.

Unit A at the base of the core (900–720 cm depth; 81 cm bmsl–99 cm amsl) correspond to the substrate. It is composed of fine ochre-coloured quartz sands with cm-scale *kurkar* aggregates. MS shows slightly negative values (ca. -10.10^-5 SI).

Unit B, located from a depth of 720 to 600 cm (100–220 cm amsl), is composed of grey fine sediments (silts and fine sands) rich in organic matter. It is characterised by fluctuation in the MS values (from -4.10^-5 SI to 470.10^-5 SI) due to changes in grain size throughout the unit and the presence of numerous ceramics (Table 3). Ostracod fauna is dominated by the freshwater ostracod *Heterocypris salina* (>60% of the total assemblage). This unit is radiocarbon dated to the Persian period (750–420 cal BC at 678 cm depth (141 cm amsl)) and 770–520 cal BC at 710 cm depth (109 cm amsl). The chronology is confirmed by the

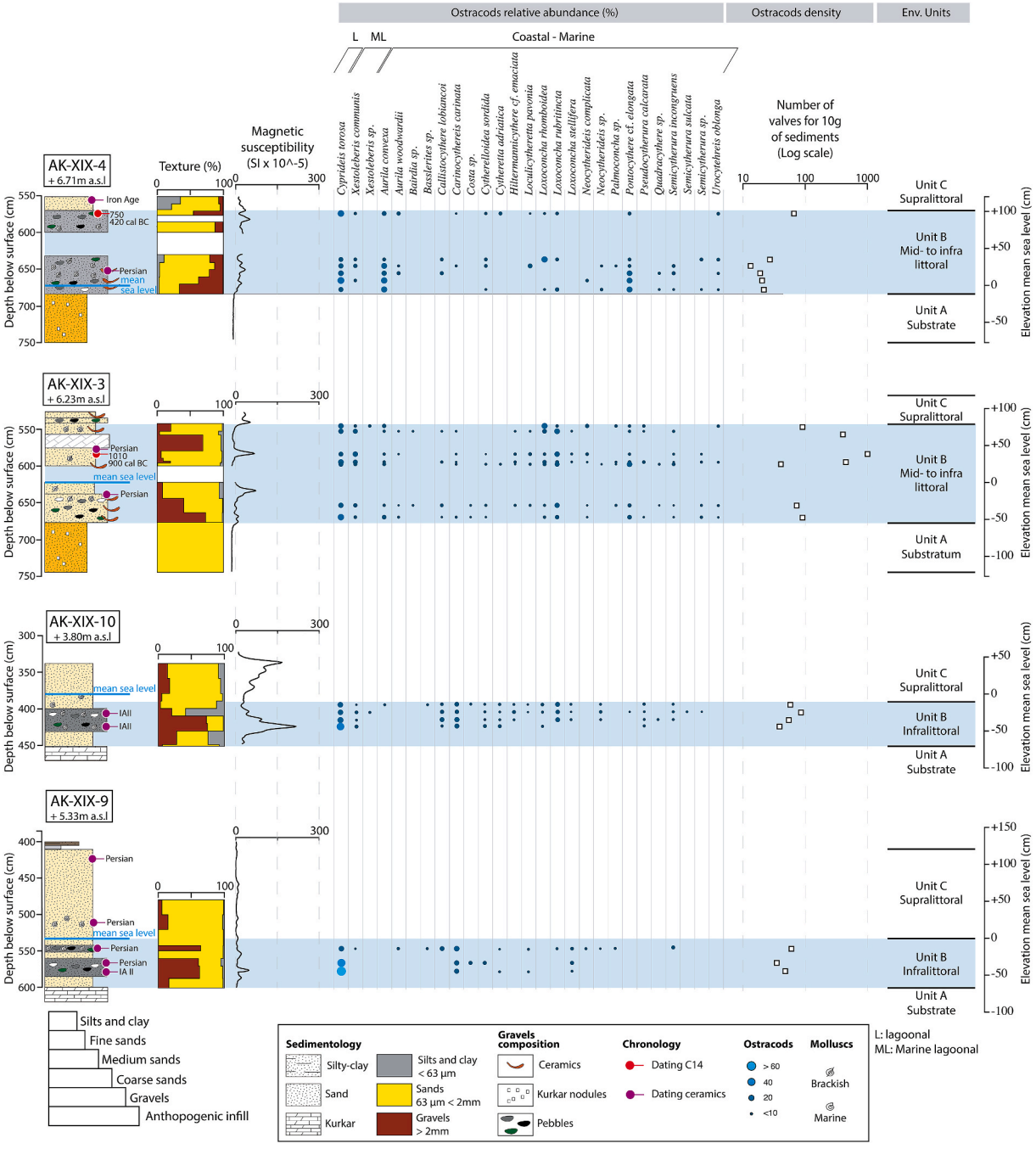


Fig. 10. Sedimentary texture, magnetic susceptibility and analysis of ostracods of cores AK-XIX-3, AK-XIX-4, AK-XIX-9 and AK-XIX-10. The different environmental units identified shows the presence of a shallow coastal environment dated to the Persian period (units highlighted in blue). See Fig. 3 for location of the cores. (For interpretation of the references to colour in this figure legend, the reader is referred to the Web version of this article.)

presence of numerous ceramic sherds in the core from the same period (Table 3). This unit containing a lot of anthropic material (charcoals, grape seeds, ceramic sherds) is interpreted as a possible sewage/drainage channel.

Unit C is a 120 cm thick sandy layer (600–480 cm depth; 220–340 cm amsl) barren of fauna and characterised by fluctuating MS values. Sherds found in this unit are dated from the Persian period. This unit may be inferred as a beach environment.

Unit D between 480 and 130 cm depth (340–790 cm amsl) is dominated by brown silty-clay sediments with a subsidiary fraction of fine sands, *kurkar* aggregates and small sherds. MS values fluctuate between 0 and 150.10^-5 SI. This unit is interpreted as an anthropogenic/agricultural soil.

Unit E, at the top of the core (130–0 cm depth), correspond to recent anthropogenic infill.

4.3.4. *Cores AK-XIX-3, AK-XIX-4, AK-XIX-9 and AK-XIX-10*

These four cores were drilled further south (Fig. 3). As for the core AK-XIX-5, their upper sections represent recent anthropogenic infills and post-habitation anthropogenic/agricultural soil. To ease visualization, the upper sections of these cores are not represented in the stratigraphic logs (Fig. 10).

Unit A in the four cores correspond to the substrate, either composed of fine quartz sands with centimetre scale *kurkar* aggregates (cores AK-XIX-3 and AK-XIX-4) or *kurkar* sandstone (cores AK-XIX-9 and AK-XIX-10).

Unit B, ranging from 50 to ca. 100 cm thick, is composed of interbedded layers of sand and small pebbles supported by a sandy matrix,

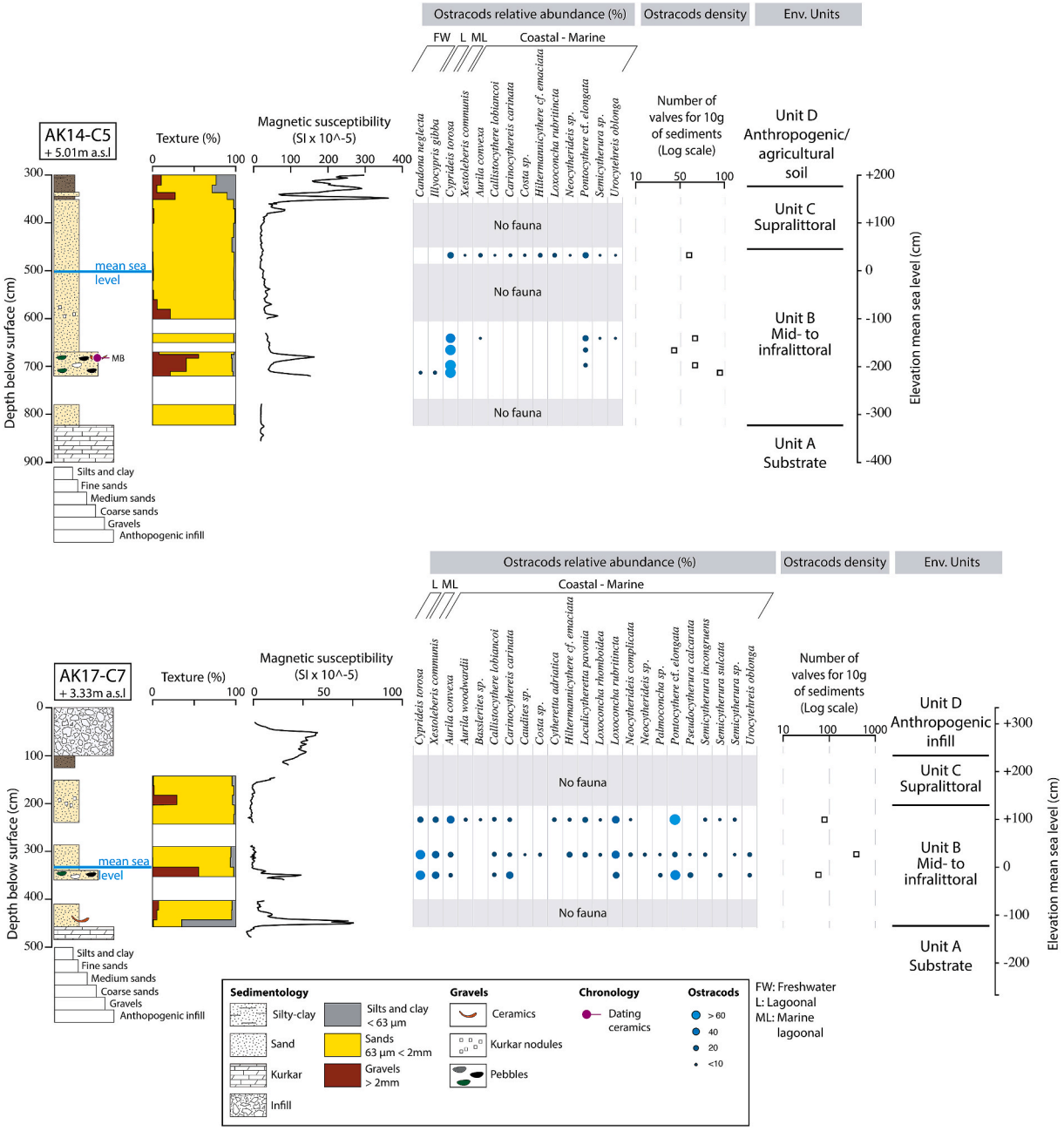


Fig. 11. Sedimentary texture, magnetic susceptibility and analysis of ostracods of cores AK14-C5 and AK17-C7. The different environmental units identified are characteristic of a coastal progradation. The infralittoral environment in which we identified marine and coastal ostracods is followed by the development of a supralittoral beach environment barren of fauna. See Fig. 3 for location of the cores.

both hosting shell fragments. MS values are relatively low, with some spikes in the MS values, probably related to the presence of ceramic-sherds and or the presence of small rounded pebbles. The sediments contain shell fragments. Well-preserved shells are scarce with a few marine (e.g. *Donax trunculus*, *Conus mediterraneus*, *Nassarius corniculus*) and brackish water (*Melanoides tuberculata*, *Melanopsis buccinoidea*) species identified. Ostracod fauna collected in the samples are representative of lagoonal (*Cyprideis torosa*), marine lagoonal (*Xestoleberis* spp.) and coastal/marine species. Among the coastal/marine groups over 20 different species were identified (e.g. *Aurila convexa*, *Loxoconcha*, *Pontocythere* cf. *elongata*; Fig. 10). Even if the diversity of species is high, the density is low with less than 100 ostracod valves per 10 g of sediment except in core AK-XIX-3 where the density reaches 500–1000 ostracod valves per 10 g of sediment. The upper part of this unit is located above present mean sea level and may only show the deposition of marine infralittoral sediments in the mid-littoral zone. This unit is radiocarbon dated from the Early Iron Age (1010–900 cal BC) in core AK-XIX-3 and from the Phoenician/Persian period (750–420 cal BC) in core AK-XIX-4. Dating of core AK-XIX-4 is in agreement with the chronology of all the four cores based on the ceramic sherds found within this unit. However, the dating in AK-XIX-3 shows a chronological gap likely due to the old wood effect of the charcoal (Table 2 and 3). Part of the ceramic sherds found within this unit attest to weathering induced in a high energy environment, associated with an ancient coastal surf zone (Figs. 2 Supplementary Material).

Unit C is composed of fine yellow quartz-rich sand barren of fauna and demonstrates the development of an emerging supralittoral environment most probably associated with the progradation of the coast at that time.

4.3.5. Cores AK14-C5 and AK17-C7

AK14-C5 and AK17-C7 were drilled in the southwest of the tell (Figs. 3 and 11). Their general stratigraphy is composed of four main units.

Unit A corresponds to the *kurkar* substrate at 8.20 m depth (3.20 m bmsl) in core AK14-C5 and 4.60cm depth (1.30 m bmsl) in core AK17-C7.

Unit B is composed of fine marine quartz-rich sands characterised by low MS values (close to 0.10^{-5} SI). Ostracod fauna is scarce with density <100 valves per 10 g of sediments. The faunal assemblage is characteristic of a coastal marine environment with lagoonal (*Cyprideis torosa*), marine lagoonal (*Xestoleberis* spp.) and coastal/marine species (e.g. *Aurila convexa*, *Loxoconcha rubrincinata*, *Pontocythere* cf. *elongata*). Two freshwater species (*Candona neglecta* and *Illyocypris gibba*) were identified in the lowermost part of the unit. A ceramic sherd dated to the Middle Bronze was found in core AK-14-C5 at 676 cm depth (175 cm bmsl). Neither marine shells nor organic material were found for radiocarbon dating. This unit is interpreted as prograding beach environment.

Unit C is composed of quartz-rich sands located 40–60 cm amsl. It is characterised by low MS values typical of well sorted quartz sands. The fauna is absent from this unit. Unit B is interpreted as a emerging beach environment.

Unit D in the uppermost part of the core (first 320 cm in AK14C5 and first 120 cm in AK17-C7) corresponds either to an anthropogenic/agricultural soil of silty-clay to sandy texture or recent anthropogenic infills.

5. Discussion

In the Iron Age – Phoenician/Persian periods – a dynamic beach environment has been shown on the western edge of Tel Akko. At the end of the Persian period, the increasing sedimentary inputs led to the progressive infilling of the area and Tel Akko lost its access to the sea.

5.1. Geomorphological setting of the western edge of Tel Akko

Multidisciplinary investigation of the western edge of Tel Akko has demonstrated that this part of the tell has been built on coastal sand dunes covering the *kurkar* bedrock as shown by the analysis of the ERT profiles and coring. Core AK-XIX-8, drilled along the ERT line Akko-1 (Fig. 3), allowed us to demonstrate that the lower resistivity areas in the upper part of the ERT profiles correspond to brown silty-clay sediments with a subsidiary fraction of fine sands, *kurkar* aggregates and small sherds, most probably related to anthropogenic/agricultural soils. Stratigraphy of the core proved that the high resistivity areas below 6 m depth, reflect the presence of a sand unit. This sand is mainly composed of very fine quartz grains and reflect aeolian deposition of sand in the area. Archaeological evidence confirms the building of city ramparts throughout the tell using this sandy substratum (Fig. 4).

Analysis of core AK-XIX-5, show the possible presence of a sewage/drainage canal to the sea west of the substantial buildings identified and where *ostraca* were found in area G (Figs. 9 and 12). The presence of the sewage is evidenced by a relatively fine sediment unit containing the ostracod *Heterocypris salina* which can inhabit brackish temporary water bodies (Fig. 9). It has also been demonstrated that *H. salina* can withstand a certain degree of organic water pollution (Mezquita et al., 1999). Furthermore, we found in this unit numerous pieces of charcoal, grapes seeds and sherds indicating the deposition of anthropogenic material originating from the tell during heavy rains in the Persian period (Table 2). An even earlier sewage/runoff drainage was found in the southern limit of the tell, under area PH, dated to the MBII thought at first to be a postern gate (secondary door or gate in a fortification; Raban, 1991), but should be identified as a sewage/drainage of the gate area of area P as it was too small to allow the passage of people (Fig. 13).

The results of the study of the cores drilled on the western and southwestern areas of Tel Akko outline the location the city's waterfront in the Phoenician/Persian period (Figs. 12 and 14). It was evidenced in the form of an exposed shallow sandy to pebbly coastal environment. Rounded sherds of imported ceramics found within the cores, show evidence of weathering by waves in the coastal surf zone and were dated to the same period (Table 3; Supplementary Material). This unit directly covers the substrate composed of *kurkar* and fine to medium quartz-rich sands probably originating from the weathering of the *kurkar* sandstone and the deposition of aeolian sands. Considering its elevation in relation to the current sea level and assuming that the relative sea level has been roughly stable since the end of the 1st Millennium BC (Sivan et al., 2001), large ships linked to interregional trade could not dock in the immediate proximity of the tell during the Persian period as the water depth would have been <50 cm (Figs. 10, 12 and 14). Moreover, we may reasonably expect a rapid infill of this area during the Late Persian period because the ceramic sherds discovered are dated from the 4th century BC at the very latest. GPR surveys shows the presence of a aggradational and progradational geomorphic environment such as a coastline in the same area.

5.2. Location of the anchorage

The beach identified at the foot of Tel Akko provided direct access to the open sea but the shallow water depth did not allow for the navigation of large vessels. Around our core AK14-C5 and further south, the area seems to have been more favourable for the anchorage of large ships during the Phoenician and Persian periods (Fig. 12). Sediment cores corroborate the interpretation of the ERT profiles. While high resistivity units correspond to relatively coarse dry sands and kurkar, lower resistivity sections (blue colour) are indicative of the presence of fine to medium sands, typical of an open marine environment on the southwest of Tel Akko (Figs. 5 and 14). Thus, the Phoenician/Persian anchorage, now landlocked, must have existed in the coastal plain located to that southwest area of the tell (Fig. 14). Persian ceramics were previously found in core AK-6 (Morhange et al., 2016, Fig. 14) at 575 cm

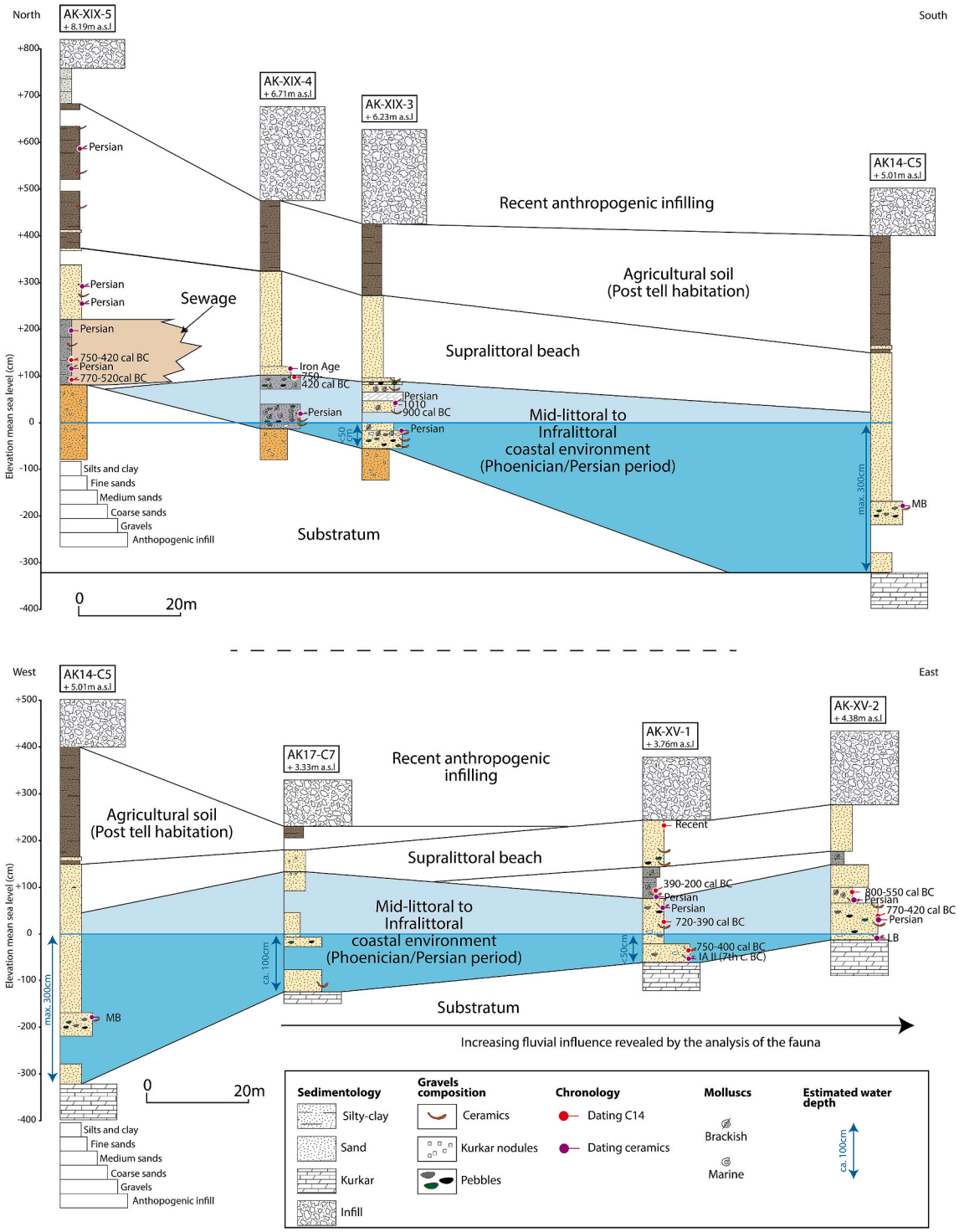


Fig. 12. Correlation of sediment cores retrieved from the west and southwest feet of Tel Akko. Location of transects is given in Fig. 3. These transects show the geomorphology of the beach environment and the variation of the water column height. The different shades of blue depict the infralittoral zone (always submerged) from the mediolittoral zone (which corresponds to the transition zone between a permanently emerged and a permanently submerged environment). C14 dating of cores AK-XV-1 and AK-XV-2 (Giaime et al., 2018) have been calibrated using the new calibration curve IntCal20 (Reimer et al., 2020). See Fig. 3 for the location of the cores. (For interpretation of the references to colour in this figure legend, the reader is referred to the Web version of this article.)

depth (200 cm below mean sea level) showing that the water column in the area neighbouring our core AK14-C5 was ca. 200 cm (Figs. 11 and 14). This depth was sufficient for the anchorage of maritime vessels (Fig. 12). An example of the boats in use along the Levantine coast in the Persian period is given by the Ma'agan Mikhael wreck, discovered ca. 40 km south of Tel Akko in 1985 (Linder and Kahanov, 2003; Kahanov and Linder, 2004). This merchant boat, radiocarbon dated to about 400 years BC, had a draft of 140 cm and a cargo capacity of 15.9 tons (Ben Zeev et al., 2009). We can reasonably assume that this kind of boat was able to approach the coast of Tel Akko with a 200 cm water depth. Moreover, goods could be safely unloaded and transported to the beach by smaller ships such as lighters or barges. Another possibility that



Fig. 13. Photo of the MBII (2000–1750 BC) postern gate in area P, from the south. Photo © M. Artzy.

cannot be excluded, is the presence of basic constructions of a proto harbour, such as small sized piers, quays or jetties in the area investigated which had facilitated the docking of boats.

5.3. Coastal progradation and abandonment of Tel Akko

Radiocarbon dating and ceramic sherds identification confirms that the sea was present in the immediate proximity of the tell until the 3rd century BC. At that time, the sedimentary inputs on the western side of Tel Akko led to the progressive infilling of the area. The fact that Tel Akko benefited from a direct access to the sea from the Bronze Age to the Late Persian/Early Hellenistic period has largely contributed to its importance in maritime activities over the centuries in the Bay of Haifa/Akko and at a larger regional scale (Artzy, 2006). The small apparent sedimentation rate in the area is in contradiction with the large sedimentation rates evidenced in the centre of the Haifa Bay. Porat et al. (2008) have estimated the progradation rate of the bay to be ~40 cm/year between 4000 and 3650 years BP (ca. 2000–1650 BC). Afterward, the coastline continued to migrate westwards at an approximate rate of 50 cm/year until present day.

In the Akko plain, sediment deposition of that volume reported by Zviely et al. (2007) and Porat et al. (2008) is not apparent. We assume that an obstacle, in the form of an aeolianite ridge (*kurkar*) identified ca. 400 m to the south of the tell could have blocked the longshore drift and the sedimentary inputs to the north (Fig. 14). This ridge probably acted as a natural coastal groyne or dyke. The relative influence of the river and marine sediment flux by longshore drift in the loss of Tel Akko's direct access to the sea is still difficult to determine precisely. However, our data point toward increasing sedimentary dynamics from marine origin in the southwestern area of Tel Akko leading to the progressive westward progradation of a sandy beach by continuous deposition of coastal sediments during the Late Persian period.

Archaeological evidence attest that Tel Akko was occupied until the beginning of the Hellenistic period (Artzy, 2015). Archaeological findings attest to extensive maritime trade reflecting the city's growth and prosperity until this period (Artzy and Be'eri, 2010). At the same time, the population began relocating to the lower city on the Akko promontory. For a few decades, Tel Akko and the new city were occupied simultaneously (3rd-2nd centuries BC).

In our work, we did not find evidence of any coastal or marine environment dated after the Late Persian/Early Hellenistic period. It seems that the main response to the increasing sedimentary input has been the relocation of the city to the Akko promontory in the Hellenistic period (Figs. 2 and 14). Rare archaeological finds dated prior to the 3rd century BC and the complete absence of Attic (Greek) imported ware, commonly widespread in the coastal region, attest that there was no

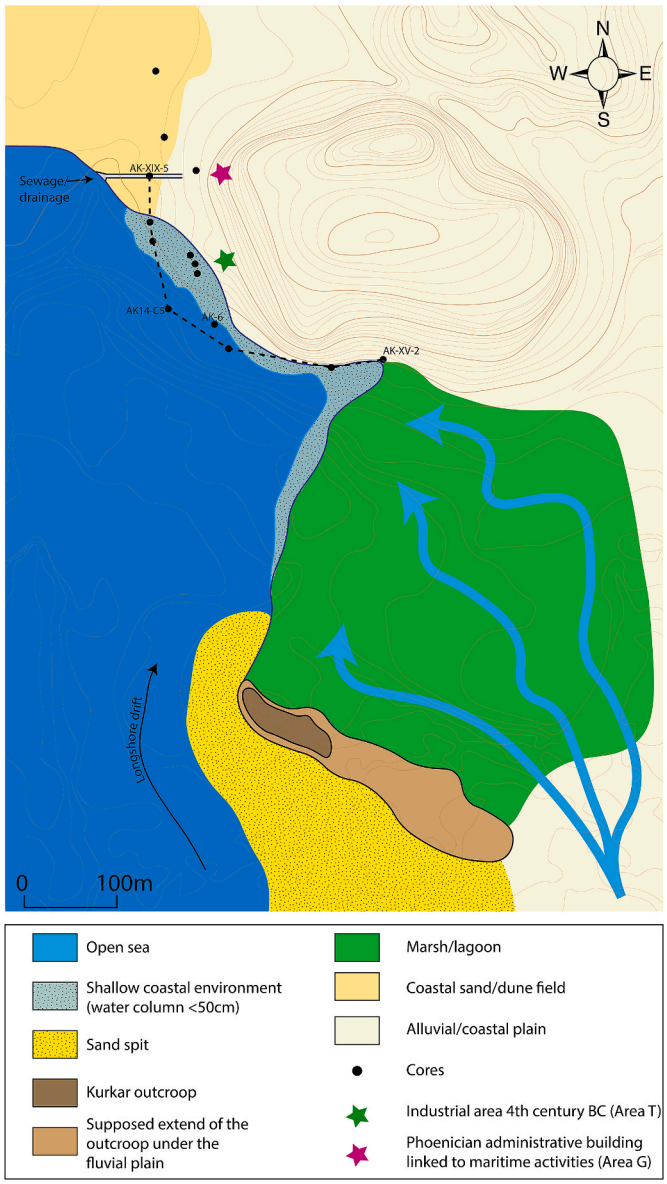


Fig. 14. Palaeoenvironmental reconstruction of Tel Akko maritime interface in the Phoenician/Persian period. The different environments have been identified based on this study and from previous research (Morhange et al., 2016; Giaime et al., 2018). The dotted line shows the location of the core transects as seen in Fig. 12. Topography was adapted from a map produced by Treidel (1925–1926).

large-scale maritime activity at a harbour in the promontory prior to the Hellenistic period (Stern et al., 2008). However, from that period, the new city benefited by a commercial (Galili and Rosen, 2017; Galili et al., 2010) and a military harbour (Sharvit et al., 2013, 2021). Intense maritime activities since the Hellenistic period were evidences during the dredging of the harbour basin (Galili et al., 2010). These findings show that the new city of Akko became the main commercial centre at the expense of the tell.

6. Conclusion

Archaeological excavations have demonstrated that Tel Akko was densely occupied and was a main maritime hub along the coast of the southern Levant during the Phoenician/Persian periods. Intensive maritime activities have been evidenced by the numerous imported ceramics and *ostraca* discovered on the tell, suggesting that at that time,

an anchorage was located in close proximity. Using a multidisciplinary approach to better understand the evolution of the Akko coastal plain to the west and southwest of Tel Akko, we were able to locate the Phoenician/Persian waterfront at the southwestern foot of the tell. We suggest that this area was the most suitable for the anchorage of boats with a water depth reaching ca. 2 m during the Persian period. We recommend future research to be focused around this specific area of the tell. The new data findings highlight the archaeological potential of the coastal plain in immediate proximity to tell and further south-southwest. Local and regional public authorities should be made aware of this new hypothesis in the event of future urban developments planned in the area.

Author contributions

M.G., H.J., Y.S., G.L. and M.A. designed the study. All the authors collected the data in the field. M.G., L.B. and A.M. carried out laboratory analyses. M.G., H.J., L.B. and M.A. analysed the resulting data. M.G., H. J. and M.A. prepared the figures and wrote the original manuscript. All the authors revised the original manuscript draft.

Data availability

Data used for the present research are detailed in the paper and its supplementary files.

Funding

This research has been carried out thanks to the support of the United States-Israel Binational Science Foundation (BSF) to the project “A Palaeo-Hydrological Approach to Understanding the Complex Coastal Evolution of an Ancient Maritime Trade City: The Tel Akko Multi-Disciplinary Case Study, Israel” to M. Artzy and H.M. Jol (Grant No. 2016080).

Declaration of competing interest

The authors declare that they have no known competing financial interests or personal relationships that could have appeared to influence the work reported in this paper.

Acknowledgements

Geoarchaeological investigations at Tel Akko have been possible thanks to permits provided by the Israel Antiquities Authority (IAA) and financial support from the BSF (2017–2020). We thank Drs. Nimer Taha and Nicolas D. Waldmann, laboratory manager and laboratory leader of the PetroLab, University of Haifa, for their analytical support and use of their facilities. M.G. thanks the Authority for Advanced Studies and the Leon H. Charney School of Marine Sciences at the University of Haifa and the BSF for the funding of his post-doctoral fellowship. H.J. thanks the University of Wisconsin - Eau Claire’s Office of Research and Sponsored Programs for Student/Faculty Research, Collaboration and Diversity mentoring Grants for Logan Bergevin and Ethan Sailer-Haugland. MA is thankful to the Hatter Foundation and an anonymous donor. We thank two anonymous reviewers for their careful reading of our manuscript and their insightful comments and suggestions.

Appendix A. Supplementary data

Supplementary data to this article can be found online at https://doi.org/10.1016/j.quaint.2021.06.008.

References

Artzy, M., 2006. The carmel coast during the second part of the late Bronze age: a center for eastern mediterranean transhipping. Bull. Am. Sch. Orient. Res. 343 (1), 45–64.
Artzy, M., 2012. Return to Tel Akko, its Anchorages, Harbour, and Surroundings, vol. 37. Recanati Institute for Maritime Studies Newsletter, University of Haifa, pp. 5–14.
Artzy, M., 2015. What is in a name? ‘Akko–Ptolemais–‘Akka–Acre. Complutum 26 (1), 205–212.
Artzy, M., Be’eri, R., 2010. Tel Akko. In: Killebrew, A.E., Raz-Romero, V. (Eds.), One Thousand Nights and Days—Akko through the Ages. Hecht Museum, Haifa, pp. 14–23.
Artzy, M., Quartermaine, J., 2014. How and when did Tel Akko get its unusual banana shape? In: Galanakis, Y., Wilkinson, T., Bennet, J. (Eds.), Αθυρματα. Critical Essays on the Archaeology of the Eastern Mediterranean in Honour of E. Susan Sherrat, 11-22. Archaeopress Archaeology, UK.
Artzy, M., Jol, H., Giaime, M., Salmon, Y., abu-Hamid, A., López, G.I., Morhange, C., Kaniewski, D., Bauman, P., Killebrew, A.K., 2021. Coastline, river changes and their effects on anchorages/harbors and habitation patterns: Akko (Israel) as an example. In: Demisticha, S., Blue, L. (Eds.), Under the Mediterranean I. Studies in Maritime Archaeology. Sidestone Press, Leiden, Netherlands, pp. 267–278.
Athersuch, J., Horne, D.J., Whittaker, J.E., 1989. Marine and brackish water ostracods (Superfamilies Cypridacea et Cytheracea): Keys et notes for the identification of the species. E.J. Brill, Leiden, The Netherlands.
Avnaim-Katav, S., Agnon, A., Sivan, D., Almogi-Labin, A., 2016. Calcareous assemblages of the southeastern Mediterranean low-tide estuaries. Seasonal dynamics and paleo-environmental implications. J. Sea Res. 108, 3049.
Beeri, R., 2008. Tel Akko and the Urbanization of Akko Plain in the First Half of the Second Millennium BCE. Unpublished PhD thesis. Department of Archaeology, University of Haifa (In Hebrew).
Ben Zeev, A., Kahanov, Y., Tresman, J., Artzy, M., 2009. The Ma‘agan Mikhael Ship: A Reconstruction of the Hull. Israel Exploration Society and Leon Recanati Institute for Maritime Studies, University of Haifa, Haifa.
Conyers, L.B., Goodman, D., 1997. Ground-penetrating Radar: an Introduction for Archaeologists. AltaMira Press.
D’Angelo, G., Garguillo, S., 1978. Guida Alle Conchiglie Mediterranee, Conoscerle, Cercarle, Collezionarle. Fabri Editori, Milan.
Dothan, M., 1976. Akko: interim excavation report first season 1973/74. Bull. Am. Sch. Orient. Res. 224, 1–48.
Dothan, M., 1985a. A Phoenician inscription from Akko. Isr. Explor. J. 35 (2/3), 81–94.
Dothan, M., 1985b. Ten seasons of excavations in ancient Akko. Qadmoniot 18, 2–24.
Elyashiv, H., Bookman, R., Zviely, D., Avnaim-Katav, S., Sandler, A., Sivan, D., 2016. The interplay between relative sea-level rise and sediment supply at the distal part of the Nile littoral cell. Holocene 26 (2), 248–264.
Empereur, J.Y., 1995. Le port hellénistique d’Amathonte. In: Karageorghis, V., Michaelides, D.D. (Eds.), Cyprus and the Sea Proceedings of the International Symposium, 131-138. University of Cyprus-Cyprus Ports Authority: Nicosia.
Empereur, J.Y., Verlinder, C., 1987. The underwater excavations at the ancient port of Amathus in Cyprus. Int. J. Naut. Archaeol. 16, 7–18.
Empereur, J.Y., Koželj, T., Picard, O., Wurch-Koželj, M., 2018. The Hellenistic Harbour of Amathus: Underwater Excavations, 1984-1986. Volume 1, Architecture and History. Études Chypriotes (19). École Française d’Athènes, Athens.
Frenzel, P., Boomer, I., 2005. The use of ostracods from marginal marine, brackish waters as bioindicators of modern and quaternary environmental change. Palaeogeogr. Palaeoclimatol. Palaeoecol. 225 (1), 68–92.
Galili, E., Rosen, B., 2017. The Akko marina archaeological project—summary. In: Galili, E. (Ed.), The Akko Marina Archaeological Project. BAR Publishing, Oxford, England, pp. 320–344. BAR International Series 2862.
Galili, E., Rosen, B., Zviely, D., Silberstein, N., Finkielsztejn, G., 2010. The evolution of Akko harbour and its Mediterranean maritime trade links. J. I. Coast Archaeol. 5, 191–211.
Gambash, G., 2014. En route to Egypt: Akko in the Persian period. J. Near E. Stud. 73 (2), 273–282.
Giaime, M., Morhange, C., Marriner, N., López, G.I., Artzy, M., 2018. Geoarchaeological investigations at Akko, Israel: new insights into landscape changes and related anchorage locations since the Bronze Age. Geoarchaeology 33 (6), 641–660.
Giaime, M., Marriner, N., Morhange, C., 2019. Evolution of ancient harbours in deltaic contexts: a geoarchaeological typology. Earth Sci. Rev. 191, 141–167.
Inman, D.L., 2003. Littoral cells. In: Schwartz, M. (Ed.), Encyclopedia of Coastal Science. The Earth Sciences Encyclopedia Online. Kluwer Academic Publishers, Dordrecht, Netherlands, pp. 594–599.
Jol, H.M., Bristow, C.S., 2003. GPR in sediments: advice on data collection, basic processing and interpretation, a good practice guide. In: Bristow, C.S., Jol, H.M. (Eds.), Ground Penetrating Radar in Sediments, 9-27. Geological Society, Special Publications, London, p. 211.
Kafri, U., Ecker, A., 1964. Neogene and Quaternary Subsurface Geology and Hydrogeology of the Zevulun Plain. Ministry of Development, Geological Survey: Israel.
Kahanov, Y., Linder, E., 2004. In: Tresman, J. (Ed.), The Ma‘agan Ship: the Recovery of a 2400-Year-Old Merchant-Man, Volume II. Israel Exploration Society and University of Haifa, Jerusalem.
Kaniewski, D., Van Campo, E., Morhange, C., Guiot, J., Zviely, D., Shaked, I., Otto, T., Artzy, M., 2013. Early urban impact on Mediterranean coastal environments. Sci. Rep. 3, 3540.
Lachenal, A.M., 1989. Écologie des ostracodes du domaine méditerranéen: Application au golfe de Gabès (Tunisie orientale), les variations du niveau marin depuis 30 000 ans, vol. 108. Documents des Laboratoires de Géologie de Lyon.
Linder, E., Raban, A., 1965. Underwater survey of Akko harbour. In: The Western Galilee and the Galilee Coast. The 19th Convention for Yediat Haaretz, Jerusalem, pp. 180–193 (In Hebrew).

Linder, E., Kahanov, Y., 2003. In: Black, E. (Ed.), The Ma'agan Mikhael Ship: the Recovery of a 2400-Year-Old Merchant-Man, vol. I. Israel Exploration Society and University of Haifa, Jerusalem.
Marriner, N., Morhange, C., Kaniewski, D., Carayon, N., 2014. Ancient harbour infrastructure in the Levant: tracking the birth and rise of new forms of anthropogenic pressure. Sci. Rep. 4, 5554.
Marriner, N., Morhange, C., Flaux, C., Carayon, N., 2017. Harbors and ports, ancient. In: Gilbert, A.S., Goldberg, P., Holliday, V.T., Mandel, R.D., Sternberg, R.S. (Eds.), Encyclopedia of Geoarchaeology. Springer Netherlands, Dordrecht, pp. 382–403.
Mezquita, F., Griffiths, H., Sanz, S., Soria, J., Piñón, A., 1999. Ecology and distribution of ostracods associated with flowing waters in the eastern iberian peninsula. J. Crustac Biol. 19 (2), 344–354.
Morhange, C., Giaime, M., Marriner, N., abu Hamid, A., Bruneton, H., Honnorat, A., Kaniewski, D., Magnin, F., Porotov, A.V., Wante, J., Zviely, D., Artzy, M., 2016. Geoarchaeological evolution of Tel Akko's ancient harbour (Israel). J. Archaeol. Sci.: Report 7, 71–81.
Pérès, J.M., 1982. Major benthic assemblages. In: Kinne, O. (Ed.), Marine Ecology, Part 1, vol. 5. Wiley, Chichester, pp. 373–522.
Pérès, J.M., Picard, J., 1964. Nouveau Manuel de Bionomie Benthique de La Mer Méditerranée. Periplus, Marseille.
Porat, N., Sivan, D., Zviely, D., 2008. Late Holocene embayment infill and shoreline migration, Haifa bay, eastern mediterranean. Isr. J. Earth Sci. 57 (1), 21–31.
Raban, A., 1983. The biblical port of Akko on Israel's coast. Archaeology 36 (1), 60–61.
Raban, A., 1985. The ancient harbours of Israel in Biblical times. Harbour Archaeology. In: Proceedings of the First International Workshop, vols. 11–44. BAR Publishing, Oxford, England.
Raban, A., 1991. The port city of Akko in the MBII. Michmanim 5, 17–34.
Raban, A., 1993. A group of imported 'east Greek' pottery from locus 46 at area F on Tel Akko. In: Heltzer, M., Segal, A., Kaufman, D. (Eds.), Studies in Archaeology and History of Ancient Israel, in Honour of Moshe Dothan. University of Haifa, Haifa, pp. 73–98.
Raban, A., Stieglitz, R.R., 1993. Phoenicians on the Northern Coast of Israel in the Biblical Period. Reuben and Edith Hecht Museum, University of Haifa, Haifa.
Reimer, P.J., Austin, W.E.N., Bard, E., Bayliss, A., Blackwell, P.G., Bronk Ramsey, C., Butzin, M., Cheng, H., Edwards, R.L., Friedrich, M., Grootes, P.M., Guilderson, T.P., Hajdas, I., Heaton, T.J., Hogg, A.G., Hughen, K.A., Kromer, B., Manning, S.W., Muscheler, R., Palmer, J.G., Pearson, C., van der Plicht, J., Reimer, R.W., Richards, D.A., Scott, E.M., Southon, J.R., Turney, C.S.M., Wacker, L., Adolphi, F., Büntgen, U., Capano, M., Fahrni, S.M., Fogtmann-Schulz, A., Friedrich, R., Köhler, P., Kudsk, S., Miyake, F., Olsen, J., Reinig, F., Sakamoto, M., Sookdeo, A., Talamo, S., 2020. The IntCal20 Northern Hemisphere radiocarbon age calibration curve (0-55 cal kBP). Radiocarbon 1–33. https://doi.org/10.1017/RDC.2020.41.
Sharvit, J., Buxton, B., Hale, J.R., Ratzlaff, A., 2021. The Hellenistic-Early Roman Harbour of Akko: preliminary finds from archaeological excavations at the foor of the southeastern seawall at Akko, 2008-2014. In: Demisticha, S., Blue, L. (Eds.), Under the Mediterranean I. Studies in Maritime Archaeology. Sidestone Press, Leiden, Netherlands, pp. 163–180.
Sharvit, J., Planer, D., Buxton, B., 2013. Preliminary findings from archaeological excavations along the foot of the southern seawall of Akko, 2008–2012 Michmanim 24, 39–40 (In Hebrew with English abstract).
Sivan, D., Gvirtzman, G., Sass, E., 1999. Quaternary stratigraphy and paleogeography of the Galilee coastal plain, Israel. Quat. Res. 51 (3), 280–294.
Sivan, D., Wdowinski, S., Lambeck, K., Galili, E., Raban, A., 2001. Holocene sea-level changes along the Mediterranean coast of Israel, based on archaeological observations and numerical model. Palaeogeogr. Palaeoclimatol. Palaeoecol. 167 (1–2), 101–117.
Stanley, J.D., Bernhardt, C.E., 2010. Alexandria's Eastern Harbor, Egypt: pollen, microscopic charcoal, and the transition from natural to human-modified basin. J. Coast Res. 26 (1), 67–79.
Stern, E., Galili, E., Rosen, B., 2008. Acco. In: Stern, E. (Ed.), The New Encyclopedia of Archaeological Excavations in the Holy Land, 24-36. Israel Exploration Society, Jerusalem. Biblical Archaeology Society: Washington, DC.
Stuiver, M., Reimer, P.J., 1993. Extended 14C database and revised CALIB radiocarbon calibration program. Radiocarbon 35, 215–230.
Stuiver, M., Reimer, P.J., Reimer, R.W., 2020. CALIB 8.2 [WWW program] at. http://calib.org. (Accessed 17 August 2020).
Thompson, R., Oldfield, F., 1986. Environmental Magnetism. George Allen & Uniwin, London.
Vachtman, D., Sandler, A., Greenbaum, N., Herut, B., 2013. Dynamics of suspended sediment delivery to the Eastern Mediterranean continental shelf. Hydrol. Process. 27, 1105–1116.
Zviely, D., Sivan, D., Ecker, A., Bakler, N., Rohrlich, V., Galili, E., Boaretto, E., Klein, M., Kit, E., 2006. Holocene evolution of the Haifa bay area, Israel, and its influence on ancient tell settlements. Holocene 16, 849–861.
Zviely, D., Kit, E., Klein, M., 2007. Longshore sand transport estimates along the Mediterranean coast of Israel in the Holocene. Mar. Geol. 237, 61–73.